# Correlation Between Low Frequency Auroral Kilometric Radiation (AKR) and Auroral Structures

Katherine A. Pazamickas*
Lycoming College
Williamsport, PA 17701
*Summer Intern
NASA/Goddard Space Flight Center
Greenbelt, MD 20771

James L. Green
NASA/Goddard Space Flight Center
Greenbelt, MD 20771

Dennis L. Gallagher
NASA/Marshall Space Flight Center
Huntsville, AL 35812

Scott Boardsen
L3 Communications Analytics Division
NASA/Goddard Space Flight Center
Greenbelt, MD 20771

Stephen Mende
U. C. Berkeley
Berkeley, CA 94720

Harald Frey
U. C. Berkeley
Berkeley, CA 94720

Bodo W. Reinisch
University of Massachusetts
Lowell, MA 01854

Submitted to *Journal of Geophysical Research*

July 28, 2005

## ABSTRACT

Auroral Kilometric Radiation (AKR) is a radio wave emission that has long been associated with auroral activity. AKR is normally observed in the frequency range from ~60 - 600 kHz. Low frequency AKR (or LF-AKR) events are characterized as a rapid extension of AKR related emissions to 30 kHz or lower in frequency for typically much less than 10 minutes. LF-AKR emissions predominantly occur within a frequency range of 20 kHz – 30 kHz, but there are LF-AKR related emissions that reach to a frequency of 5 kHz. This study correlates all instances of LF-AKR events during the first four years of observations from the IMAGE spacecraft's Radio Plasma Imager (RPI) instrument with auroral observations from the wideband imaging camera (WIC) onboard IMAGE. The correlation between LF-AKR occurrence and WIC auroral observations shows that in the 295 confirmed cases of LF-AKR emissions, bifurcation of the aurora is seen in 74% of the cases. The bifurcation is seen in the dusk and midnight sectors of the auroral oval, where AKR is believed to be generated. The polarization of these LF-AKR emissions has yet to be identified. Although LF-AKR may not be the only phenomena correlated with bifurcated auroral structures, bifurcation will occur in most instances when LF-AKR is observed. The LF-AKR emissions may be an indicator of specific auroral processes sometimes occurring during storm-time conditions in which field-aligned density cavities extend a distance of perhaps 5-6 $R_E$ tailward from the Earth for a period of 10 minutes or less.


## 1. INTRODUCTION

Over 30 years ago it was recognized that auroral kilometric radiation (AKR) is correlated with discrete auroral arcs [*Gurnett*, 1974]. AKR is caused by high-energy particles streaming towards the Earth along auroral field lines. AKR emissions normally occur in the frequency range between 60 and 600 kHz, with a peak in emission intensity around 200 kHz. Under certain conditions, AKR is a sensitive and reliable indicator of magnetic substorms [*Voots and Gurnett*, 1977]. While the precipitating electron-driven mechanism, responsible for the generation of AKR is inefficient and able only to convert ~0.1% of the total electron energy into wave power, the average radio wave power of a

typical AKR event is still about 1-million Watts. The rest of the energy, typically measuring in excess of 1-Gigawatt, is dumped into the aurora forming discrete auroral arcs [*Gurnett*, 1974]. AKR source regions have also been identified with particular magnetic field-lines that map into the aurora zone (assuming extraordinary mode emission) and originate from the cyclotron resonant altitudes on magnetic field lines [*Huff et al.*, 1988]. In a study by *Imhof et al.* [2004], correlations were made between both low frequency and high frequency AKR along with X-rays emissions from the auroral zone. When studying shorter time scale variations, low frequency AKR (LF-AKR), correlated better than the high frequency AKR with the intensity of the X-ray auroral emissions. However, when X-ray flux peaks near midnight, or right before dawn, LF-AKR does not correlate well. When there was a sharp increase in X-ray auroral intensity, high frequency AKR precedes the X-ray increase, while LF-AKR trails in time. *Imhof et al.* [2004] concludes that the auroral acceleration region must start at lower altitudes and move tailward. The purpose of this paper is to identify the connection between the generation of LF-AKR and the structure of the nightside aurora, generated by electron precipitation, and to find the low frequency limit of AKR related emission.

## 2. INSTRUMENTS USED

The data used in this study are from the Radio Plasma Imager (RPI) and the Wideband Imaging Camera (WIC) on the Imager for Magnetopause-to Aurora Global Exploration (IMAGE) spacecraft. IMAGE was launched on 25 March 2000, and was placed into an elliptical polar orbit, having an apogee altitude of 7.2 $R_E$, and a perigee altitude of 1000 km.

The RPI can passively record radio frequency measurements as a function of time from 3 kHz to 3 MHz, but is typically programmed to measure 3 kHz to 1 MHz electric fields [*Reinisch et al.*, 2000]. The RPI instrument alternates between passive radio wave measurements and radio sounding measurements on a time scale of about 2 minutes. These two modes of operation are analyzed and displayed differently. The passive radio wave measurements are displayed in frequency versus time spectrograms and the radio sounding measurements in plasmagrams of echo virtual range versus frequency. AKR is routinely observed by RPI during its passive radio measurements.

WIC is designed to create broad-band ultraviolet global images [*Mende et al.*, 2000] of the auroral oval at wavelengths of 140-190 nm corresponding to energetic electron precipitation and is therefore vital for evaluating auroral structure and development over time with LF-AKR. Since WIC captures an image of the auroral zone once every spin (~2 minutes) the RPI passive electric field and WIC auroral measurements are on approximately the same time scale.

## 3. EXAMPLES OF LF-AKR WITH AURORA

It is well known that the onset of AKR emissions are well correlated with the onset of auroral substorms [*Liou et al.*, 2000]. In this section we will show examples of the correlation between LF-AKR and auroral emissions. Figure 1 is composed of RPI spectrogram data with simultaneous WIC images of the auroral zone for April 28, 2002. During the main AKR burst, the emission begins shortly after 0800 UT. As shown in the corresponding WIC image, a brightening area appears in the dusk sector of the oval, which is an indication of substorm onset. As the emission continues in time, the oval activity is observed to increase in intensity and is expanding poleward. Shortly before 0830 UT, AKR (or AKR related emission) extends downward in frequency to 20 kHz, and by 0834:48 UT, a distinct secondary poleward arc, extending in latitude, appears. The aurora has bifurcated. Just before 0845 UT, AKR has reached a frequency of 12 kHz, and by 0847:06 UT, the split or bifurcation in the aurora has moved poleward. The emission continues until 0915 UT at which time the oval has begun to recover and the arc begins to fade.

Later on April 28, 2002 there is another AKR burst, as shown in Figure 2. This burst begins about 1100 UT, and at 1102:19 UT substorm onset begins, as indicated by the brightened area in the dusk sector of the oval. As the emission continues, the oval shows the expansion phase of substorm development as it moves poleward. Between 1115 and 1130 UT, AKR has reached very low frequencies and by 1126:54 UT, the aurora has begun to bifurcate. Between 1130 UT and 1145 UT, AKR reaches 12 kHz and the arc brightens and thickens. The AKR emission ends shortly after 1200 UT but not

before reaching a frequency of 20 kHz with corresponding WIC images showing an auroral arc expanding near the midnight sector.

In the May 10, 2002 event, as shown in Figure 3, the AKR emission turns on and off several times before extending down into the lower frequencies. A band of Z mode radiation is also observed extending from about 6 to 20 kHz across the entire time period. At about 0737 UT, a bright spot appears on the auroral oval, indicating magnetospheric substorm onset. AKR emission frequency is at about 90 kHz. By 0743 UT, the AKR emission intensifies, and the bright spot in the dusk sector of the oval has extended and increased in intensity. The Z mode emission first reaches 6 -7 kHz near 0749 UT, at the time the WIC image shows a secondary arc forming. By 0755 UT, AKR has intensified and extends downward in frequency to about 20 kHz. The arc has bifurcated from the oval and has extended over the entire dusk sector. The 0801 UT WIC image shows poleward movement of this now separate auroral structure corresponding to the occurrence of LF-AKR and intense Z mode emissions. By 0814 UT, the LF-AKR and the Z-mode emission have subsided and the bifurcation of the aurora is easily identified as it continues to expand poleward. The AKR emission is over by 0820 UT, while the bifurcation in the aurora has extended over the entire nightside of the oval, although it has begun to decrease in intensity. The Z mode enhancement is not always observed in coincidence with the LF-AKR.

## 4. STATISTICAL RESULTS

RPI spectrograms spanning from shortly after the launch of IMAGE starting in May 2000 through July 2004 were examined for all periods when AKR emission was observed and when AKR or an AKR related emission were found to extend below 30 kHz. AKR emissions occur in intense, well defined source regions along auroral field lines in the northern and southern hemispheres, from 22 magnetic local time (MLT) to 24 MLT, and between 2 $R_E$ and 4 $R_E$ with emissions lasting from several minutes to several hours [*Gallagher and Gurnett*, 1979]. The radiation is beamed into large emission cones [*Green et al.*, 1977; *Gallagher and Gurnett,* 1979; *Green and Gallagher*, 1985]. AKR has a normal frequency range of ~60-600 kHz, with the average peak in emission intensity

around 200 kHz (which is dependent on season). Once again, low frequency AKR is defined as AKR (or what appears to be an AKR related emission) with a frequency range of less than 30 kHz. Out of the 4312 AKR events that were identified, 669 were considered LF-AKR events. When AKR is observed by RPI, 84% of the time it appears within the typical emission frequency range. Only 16% of the time are extensions of the AKR emission band to low frequency found to occur as shown in Figures 1, 2 and 3.

Figure 4 shows all positions of the IMAGE spacecraft when LF-AKR events are observed. Figure 4 Panel A is a magnetic latitude (MLAT) versus magnetic local time (MLT) polar plot of spacecraft location all LF-AKR events. If we assume that the LF-AKR source is located along the auroral field line near 22 MLT an axis of symmetry can be identified where data can be split into primarily nightside (red) and primarily dayside (blue events). Panel B is a projection of the locations where LF-AKR is observed into a meridianal plane centered on the nightside at 22 MLT. Spacecraft latitude and radial distance is plotted in each hemisphere. The resulting display collectively shows those locations to which LF-AKR emission has access. The inset in Panel B [adapted from *Gallagher and Gurnett*, 1979] illustrates the average AKR emission cone. The distribution of the events derived here compares well with the previously derived AKR emission cone (inset) clearly indicating that there is no particular beaming pattern distribution or preferred location for observing LF-AKR events. LF-AKR appears to illuminate the entire time-averaged emission cone.

Out of the 669 LF-AKR events, suitable WIC images were only available in 295 cases. A seasonal histogram of when these events occurred is shown in Figure 5. LF-AKR emissions occur more often in the spring, maximizing during the months of May and June, as shown in Figure 5. Within this 295 event subset of LF-AKR events, bifurcation of the aurora was observed in 74% of the cases.

The localized brightening of the aurora and formation of a bifurcated auroral arc appear to suggest increased precipitation flux or energy and perhaps a topological change in the magnetic field that extends tailward from the nightside aurora. Figure 6 shows that LF-AKR is found at lower frequencies for positive dipole tilt (toward the sun). LF-AKR emissions occur more frequently in the spring, maximizing in May and June.

## 5. DISCUSSION

It is well established that AKR is generated by the cyclotron maser instability, with the emission Doppler shifted above the local RX cutoff where the radiation propagates in the free space mode from an auroral density cavity [*Wu and Lee*, 1979]. AKR emissions are observed only in regions where the local electron gyrofrequency and the local electron plasma frequency are below the wave frequency [*Green*, 1981].

The observed AKR spectrum has been used by a number of authors [see for example: *Lee et al.*, 1980; *Green et al.*, 2004] to estimate the altitude range of the source region based on the Doppler shifted gyroemission mechanism. *Green et al.*, [2004] used average AKR spectra to locate the AKR source region extent from IMAGE and Polar passive radio wave measurement observations with season. These authors report average AKR spectra ranging from 60-600 kHz and that the AKR source altitude is typically higher in summer than in the winter. It is important to note the LF-AKR events are of such short duration that they are missed in long-term statistical studies such as this.

For AKR to occur at unusually low frequencies (less than 30 kHz), the auroral flux tubes must become evacuated to higher altitude than commonly occurs as illustrated in Figure 7. Figure 7 Panel A shows the electron plasma frequency, the electron gyrofrequency, and RX cutoff frequency along the auroral field-line that contains the AKR source region. AKR requires the development of a narrow field-aligned density cavity for wave generation [*Wu and Lee, 1979*]. Note the extreme drops in density at altitudes from 3.5 to 5 $R_E$ necessary for the AKR source region to be able to generate LF-AKR. Figure 7 Panel B shows the corresponding location of the expanded AKR source into the low frequency region. Normally, AKR is thought to originate on auroral field lines out to a geocentric distance of about 3 $R_E$. For LF-AKR emission to be generated through the Doppler shifted cyclotron MASER instability as low in frequency as 5 kHz means the field-aligned density cavity must sometimes extend to nearly twice the normal distance for time periods of tens of minutes and less.

During LF-AKR events, the initial bright auroral spot usually evolves into either a narrow intense arc within the oval or a thickened but less bright area extending poleward from the oval. By the end of a LF-AKR event either a fully formed bifurcated auroral structure has appeared or the start of a brightened arc, has appeared that later moves

poleward and becomes separate from the lower latitude oval. As the primary aurora arc grows, the secondary arc begins to fade. We find no systematic correspondence between AKR intensity or the lowest frequency extent of AKR and the apparently related auroral feature intensity.

The AKR related auroral density cavity is associated with the development of an electric field parallel to magnetic field lines that accelerates electrons and greatly lowers the density in a latitudinally narrow region. The formation of a poleward auroral arc means a new, higher latitude parallel electric field has formed to cause the presence of the arc. The mechanisms that lead to the formation of a second auroral arc and apparent extension of the associated density cavity to significantly higher altitude remain to be explained.

## 6. CONCLUSION

In this study, AKR has been surveyed using IMAGE RPI and WIC observations from May 2000 through July 2004. In total, RPI spectrograms showing natural radio wave emissions have been examined for 1422 IMAGE spacecraft orbital passes. In these spectrograms 4312 separate occurrences of AKR event periods were found. Among these periods, 669 occurrences of LF-AKR were found. For these event times, suitable WIC images have been found in only 295 of the cases. In 217 of these correlated cases a separate auroral arc is clearly visible in WIC images and found to have formed poleward of the primary auroral display. Bifurcated auroral arcs are however seen at other times and consequently do not appear to be uniquely associated with LF-AKR events. The most common scenario seen in RPI and WIC observations is that a bright spot on the oval is seen at the time of the emission containing the onset of LF-AKR. The events studied here reveal that AKR can extend to frequencies lower than 20 kHz with Z mode related emissions, being observed on some occasions, reaching from 6 to 20 kHz. This extreme low frequency excursion of the AKR spectrum is indicative of a source region location at much higher altitudes than previously suggested. The implication is that there may be aspects of the morphology for AKR emission that is not yet understood. The bifurcation in the aurora is seen in a majority of cases where confirmed low frequency AKR emission reaches 30 kHz or lower, suggesting evidence of a new, direct correlation

between these waves and a particle phenomena. The two events noted in which a different auroral arc morphology appears to be related to the occurrence of LF-AKR is a preliminary identification that is not yet understood.

## 7. Acknowledgements

This research was supported by the National Aeronautics and Space Administration (NASA) at the University of Massachusetts, Lowell from subcontracts to Southwest Research Institute under contract NASW-97002. One of us, K.A.P. performed this work while a summer intern at NASA/GSFC.

## REFERENCES

Gallagher, D.L. and Gurnett, D.A., Auroral kilometric radiation: Time-averaged source location, *J. Geophys. Res.*, *84*,1979.

Green, J.L., S. Boardsen, S.F. Fung, H. Matsumoto, K. Hashimoto, R.R. Anderson, B.R. Sandel and B.W. Reinisch, Association of kilometric continuum radiation with plasmaspheric structures, J. Geophys. Res., *109* (A03203), doi:10.1029/2003JA010093, 2004.

Green, J.L., D.A. Gurnett, and S.D. Shawhan, The angular distribution of auroral kilometric radiation, *J. Geophys. Res.*, *82*, 1977.

Green, J.L., D.A. Gurnett, and R.A. Hoffman, A correlation between auroral kilometric radiation and inverted V electron precipitation, *J. Geophys Res.*, 84, 1979.

Green, J. L., "Observations pertaining to the generation of auroral kilometric radiation," The formation of auroral arcs, American Geophysical Union Monograph *25*, 359-368, 1981.

Green. J.L. and D.L. Gallagher, The detailed intensity distribution of the AKR emission cone, *J. Geophys. Res.*, *90*, 9641-9649, 1985.

Green, J.L., S. Boardsen, L. Garcia, S.F. Fung and B.W.Reinisch, Seasonal and solar cycle dynamics of the auroral kilometric radiation source region, *J. Geophys. Res.*, *109* (A052231), doi: 1029/2003JA010311, 2004.

Gurnett, D.A., The Earth as a radio source: Terrestrial kilometric radiation, *J. Geophys.*

*Res.*, *70*, 1974.

Huff, R.L., W. Calvert, J.D. Craven, L.A. Frank and D.A. Gurnett, Mapping of auroral kilometric radiation sources to the aurora, *J. Geophys. Res.*, *93*,1988.

Imhof, W.L., S.M. Petrinec, R.R.Anderson, M. Walt, J. Mobilia, Correlations between Low frequency and high frequency auroral kilometric radiation plasma wave intensity bursts and X-rays in the auroral zone, *J. Geophys. Res.*, *109* (A09204), doi: 10.1029/2003JA010357, 2004.

Lee, L.C., J.R. Kan, and C.S. Wu, Generation of auroral kilometric radiation and the structure of auroral acceleration region, *Planet Space Si*, 28, 703-711, 1980.

Liou, K., C.-I Meng, A.T.Y. Lui, and P.T. Newell, Auroral kilometric radiation at substorm onset, *J. Geophys. Res.*, *8,* 25325-25331, 2000.

Mende, S.B., H. Heetderks, H.U. Freys, J.M. Stock, M. Lampton, S.P. Geller, R. Abiad, O.H.W. Siegmund, S. Habraken, E. Renotte, C. Jamar, P. Rochus, J.C. Gerard, R. Siglerand, H. Lauche, Far ultraviolet imaging from the IMAGE spacecraft: 2, Wideband FUV imaging. Space Science Reviews, *91*, 271-286, 2000.

Reinisch, B. W., D. M. Haines, K. Bibl, G. Cheney, I. A. Galkin , X. Huang, S. H. Myers, G. S. Sales, R. F. Benson, S. F. Fung, J. L. Green, W. W. L. Taylor, J.-L. Bougeret, R. Manning, N. Meyer-Vernet, M. Moncuquet, D. L.Carpenter,, D. L. Gallagher, and P. Reiff, The Radio Plasma Imager investigation on the IMAGE spacecraft, *Space Science Reviews*, IMAGE special issue, *91*, 319-359, February, 2000.

Voots, G.R. and D.A. Gurnett, Auroral kilometric radiation as an indicator of auroral magnetic disturbances, *J. Geophys. Res.*, 82, 1977.

Wu, C.S., Lee, L.C., A theory of the terrestrial kilometric radiation, *Ap. J.*, 621-626, 1979.

## FIGURE CAPTIONS

**Figure 1.** The onset of LF AKR appears to coincide with the formation of a bifurcated auroral arc poleward of the auroral oval. The arc fades towards the end of the AKR emission event.

**Figure 2.** In this example, a bright nightside auroral spot is accompanied by the onset of AKR at 1100 UT. The extension of AKR to low frequencies appears to coincide with the development of a bifurcated aurora from 1115 to 1145 UT.

**Figure 3.** This particularly intense AKR emission begins with typical emission properties, but quickly transitions to LF-AKR. A Z mode radiation band is observed from 6 to about 20 kHz. This example highlights the need to be somewhat careful calling the emission below 20 kHz, in this event, LF-AKR.

**Figure 4.** Panel A is a magnetic latitude (MLAT) versus magnetic local time (MLT) polar plot of all LF-AKR events. Assuming that the LF-AKR source is along auroral field line at about 22 MLT as an axis of symmetry the data can be split into primarily nightside (red) and primarily dayside (blue events). Panel B shows the time-averaged extent of the cone-like emission pattern assuming that same symmetry pattern as in Panel A. The inset in Panel B [adapted from *Gallagher and Gurnett*, 1979] illustrates the average AKR emission cone. The distribution of LF-AKR events matches the AKR emission cone.

**Figure 5.** A histogram of all LF-AKR events observed by IMAGE. LF-AKR emissions occur more often in the spring, maximizing in the months of May and June.

**Figure 6.** The low frequency extent of AKR is shown in a scatter plot against the dipole tilt angle. Positive tilt is toward the sun. LF-AKR is found at lower frequencies for positive dipole tilt. As the tilt angle goes negative from zero, the minimum frequency rises.

**Figure 7.** Panel A shows the expected electron plasma frequency ($f_p$), electron gyrofrequency ($F_g$), and resulting RX cutoff frequency ($f_R$) along an auroral field line that contains the AKR source region. Panel B shows the expected AKR source region in a meridian plane. AKR is believed to be a Doppler shifted gyro emission above the local RX cutoff. The yellow highlighted region (in Panels A and B) shows how the AKR source must extend tailward in order for unusual LF-AKR to be generated.

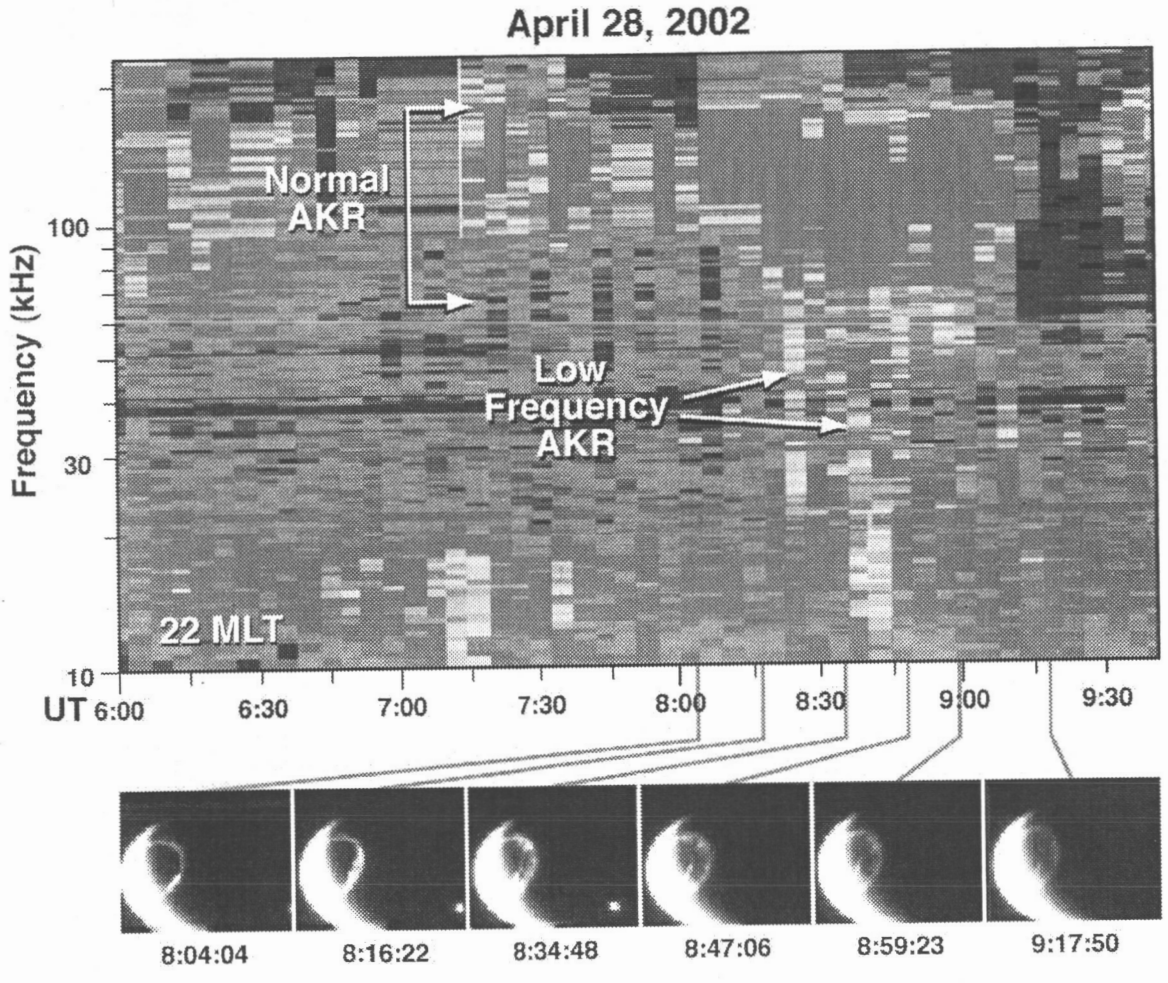
April 28, 2002
Normal AKR
Low Frequency AKR
22 MLT
Frequency (kHz)
100
30
10
UT 6:00
6:30
7:00
7:30
8:00
8:30
9:00
9:30
8:04:04
8:16:22
8:34:48
8:47:06
8:59:23
9:17:50

Figure 1

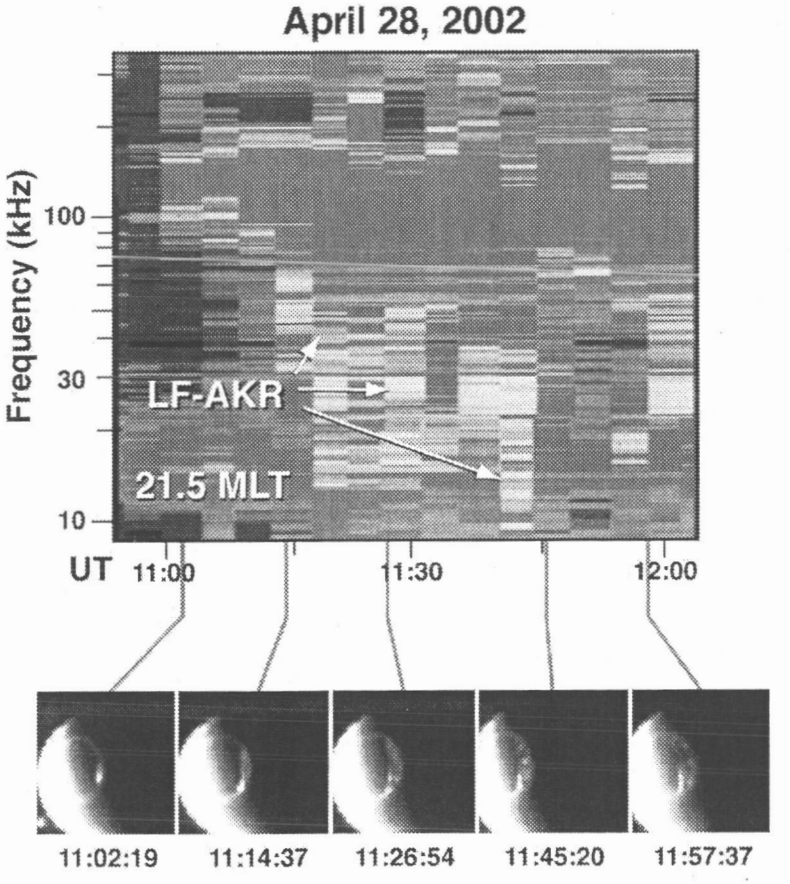
April 28, 2002
Frequency (kHz)
100
30
10
LF-AKR
21.5 MLT
UT
11:00
11:30
12:00
11:02:19
11:14:37
11:26:54
11:45:20
11:57:37

Figure 2

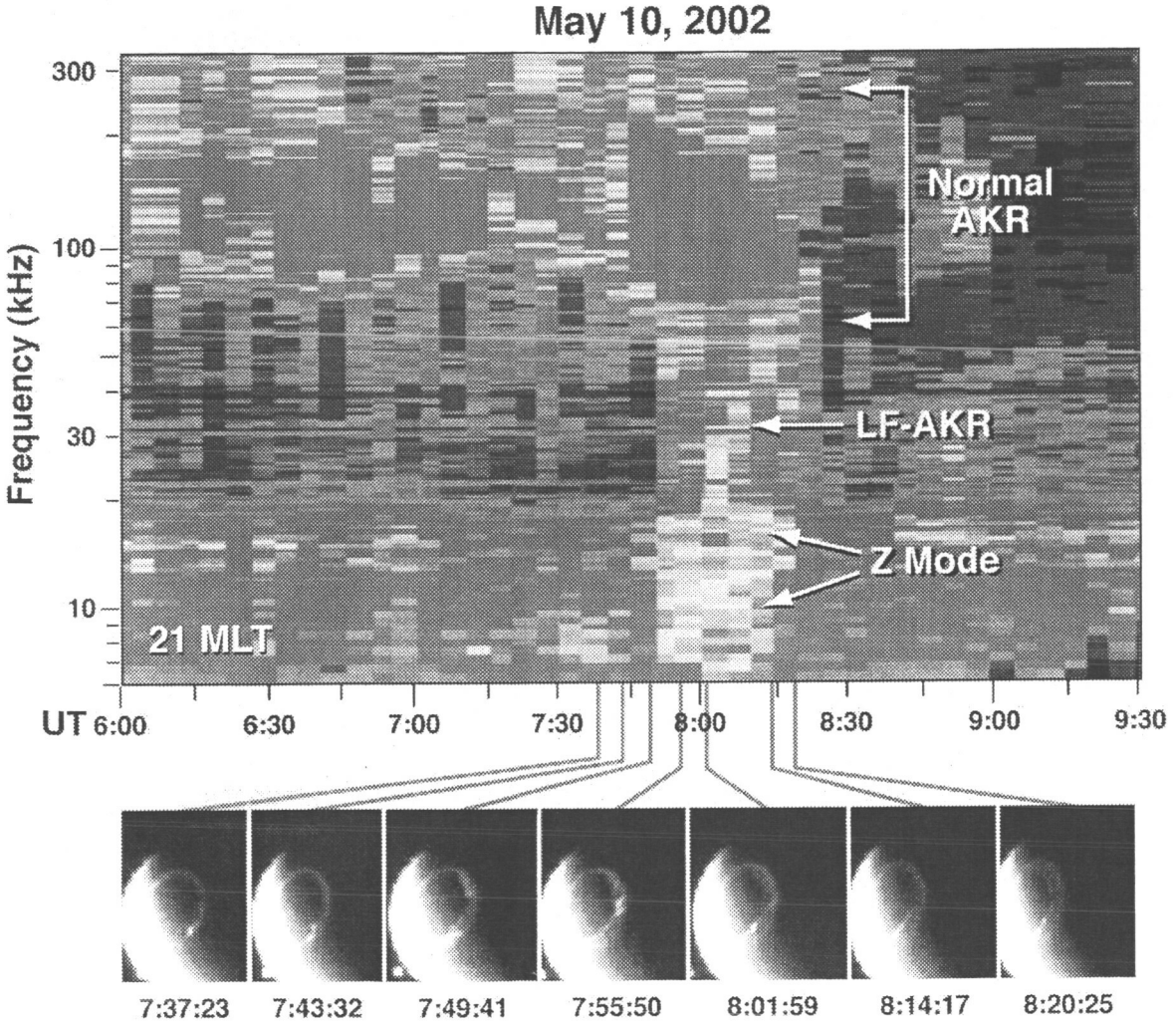
May 10, 2002
300
100
30
10
Frequency (kHz)
Normal AKR
LF-AKR
Z Mode
21 MLT
UT 6:00
6:30
7:00
7:30
8:00
8:30
9:00
9:30
7:37:23
7:43:32
7:49:41
7:55:50
8:01:59
8:14:17
8:20:25

Figure 3

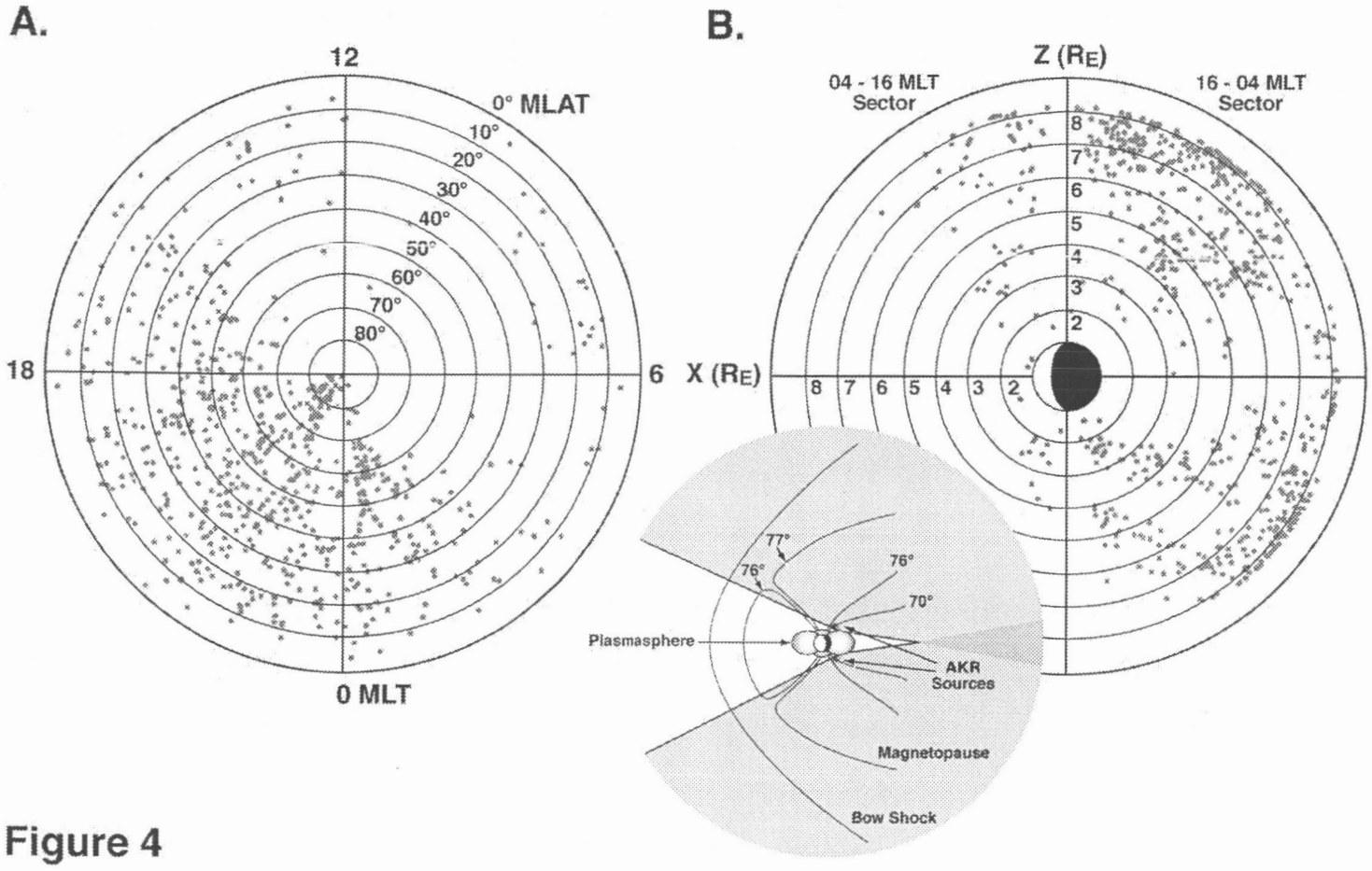
A.
12
0° MLAT
10°
20°
30°
40°
50°
60°
70°
80°
18
6
0 MLT
B.
Z (RE)
04 - 16 MLT
Sector
16 - 04 MLT
Sector
X (RE)
8
7
6
5
4
3
2
77°
76°
76°
70°
Plasmasphere
AKR
Sources
Magnetopause
Bow Shock

Figure 4

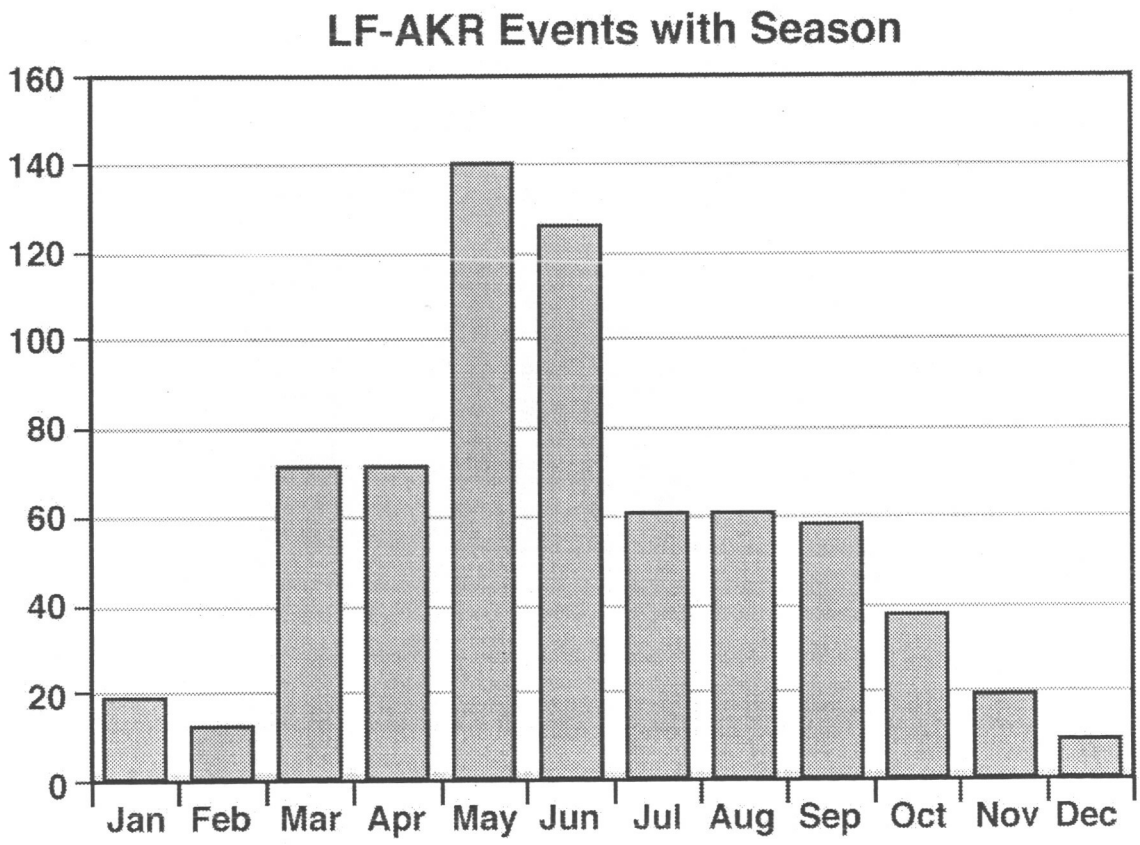
LF-AKR Events with Season
160
140
120
100
80
60
40
20
0
Jan
Feb
Mar
Apr
May
Jun
Jul
Aug
Sep
Oct
Nov
Dec

Figure 5

Science-PAO Committee

# Correlation Between Low Frequency Auroral Kilometric Radiation (AKR) and Auroral Structures

Katherine Pazamickas, James Green, Dennis Gallagher,
Scott Boardsen, Stephen Mende, Harald Frey Bodo Reinisch

Submitted to *Journal of Geophysical Research*

ABSTRACT

Auroral Kilometric Radiation (AKR) is a radio wave emission that has long been associated with auroral activity. AKR is normally observed in the frequency range from ~60 - 600 kHz. Low frequency AKR (or LF-AKR) events are characterized as a rapid extension of AKR related emissions to 30 kHz or lower in frequency for typically much less than 10 minutes. LF-AKR emissions predominantly occur within a frequency range of 20 kHz – 30 kHz, but there are LF-AKR related emissions that reach to a frequency of 5 kHz. This study correlates all instances of LF-AKR events during the first four years of observations from the IMAGE spacecraft's Radio Plasma Imager (RPI) instrument with auroral observations from the wide-band imaging camera (WIC) onboard IMAGE. The correlation between LF-AKR occurrence and WIC auroral observations shows that in the 295 confirmed cases of LF-AKR emissions, bifurcation of the aurora is seen in 74% of the cases. The bifurcation is seen in the dusk and midnight sectors of the auroral oval, where AKR is believed to be generated. The polarization of these LF-AKR emissions has yet to be identified. Although LF-AKR may not be the only phenomena correlated with bifurcated auroral structures, bifurcation will occur in most instances when LF-AKR is observed. The LF-AKR emissions may be an indicator of specific auroral processes sometimes occurring during storm-time conditions in which field-aligned density cavities extend a distance of perhaps 5-6 $R_E$ tail-ward from the Earth for a period of 10 minutes or less.